



# Selective oxidation of benzylic alcohols *via* synergistic bisphosphonium and cobalt catalysis†

 Cite this: *Chem. Commun.*, 2023, 59, 4055

 Received 6th February 2023,  
 Accepted 7th March 2023

DOI: 10.1039/d3cc00532a

rsc.li/chemcomm

 Jia Ding,<sup>‡,ab</sup> Shuaishuai Luo,<sup>‡,ab</sup> Yuanli Xu,<sup>c</sup> Qing An,<sup>a</sup> Yi Yang<sup>id</sup>\*<sup>c</sup> and  
 Zhiwei Zuo<sup>id</sup>\*<sup>b</sup>

**A synergistic photocatalytic system using a bisphosphonium catalyst and a cobalt catalyst has been developed, enabling the selective oxidation of benzylic alcohols under oxidant-free and environmentally benign conditions. High efficiencies have been obtained for a variety of alcohol substrates, and exclusive selectivity for aldehyde products has been achieved across the board. Furthermore, this photocatalytic system proved to be efficient when performed under continuous-flow conditions, even using a simple and easily assembled continuous-flow setup.**

Central to the recent emergence of photoredox catalysis, the development of photocatalysts has played a critical role in achieving novel and sustainable transformations.<sup>1</sup> Organophosphorus molecules have long been recognized for their unique electronic properties and optical behaviour.<sup>2,3</sup> Despite extensive research in organic electronics, fluorescence imaging and optical sensing, the utilization of organophosphorus compounds in photoredox catalysis remains largely underdeveloped compared with other types of organic chromophore such as acridinium dyes.<sup>4–9</sup> Photoexcited bisphosphonium **3**, which can be easily prepared from 2,2'-bis(diphenylphosphino)-1,1'-binaphthyl (BINAP),<sup>10</sup> showcases an outstanding oxidizing capacity in comparison with the most commonly used Mes-Acr<sup>+</sup> photocatalyst; nevertheless, only limited examples have been reported that include the oxidative cyclization of alkenes and the polymerization of vinyl ethers.<sup>11–13</sup> The synergistic incorporation of photocatalysts with transition metal catalysts has emerged as a powerful platform to expand the synthetic

realm of radical-mediated transformations.<sup>14</sup> Herein, we report the first synergistic catalytic system using a bisphosphonium photocatalyst and a cobalt catalyst for the selective photocatalytic oxidation of benzylic alcohols.

The selective oxidation of alcohols to aldehydes and ketones is an essential process in organic synthesis, which constantly drives the development of new catalytic strategies to achieve higher levels of efficiency and economic value under environmentally benign and practical conditions.<sup>15–17</sup> Eminently, the photochemical hydrogen evolution strategy has enabled the development of efficient dehydrogenation processes under oxidant-free and ambient conditions, enabling the oxidation of alcohols in an atom-economical fashion with molecular hydrogen as the sole side product.<sup>18–30</sup> Recently, Wu and co-workers have developed dual catalytic systems with nickel ions acting as the proton reduction catalyst and CdSe quantum dots or eosin Y being used as the photocatalyst, achieving the selective oxidation of benzylic alcohols in aqueous medium.<sup>31,32</sup> Kanai, Mitsunuma and co-workers recently demonstrated a triple catalytic system employing a Mes-Acr<sup>+</sup> photocatalyst, a nickel catalyst and a thiophosphate organocatalyst to oxidize aliphatic secondary alcohols into ketones.<sup>33</sup> Considering the synthetic utility of alcohol oxidation reactions and the commonly encountered scalability problem with photocatalytic transformations,<sup>34</sup> efficient photocatalytic systems that are adaptable in continuous flow conditions remain in high demand. Here we disclose a practical bisphosphonium/Co catalytic system that can enable the selective oxidation of benzylic alcohols in batch as well as continuous-flow conditions (Fig. 1).

*p*-Fluorobenzylic alcohol was initially chosen as the template substrate to initiate reaction optimization. Under the irradiation of LED light (light intensity: 2.5 W cm<sup>-2</sup>, λ<sub>max</sub> = 400 nm), a variety of photocatalysts were examined with the commonly utilized H<sub>2</sub> evolution catalyst Co<sup>III</sup>(dmgH)<sub>2</sub>pyCl.<sup>35</sup> As demonstrated in Fig. 2, the use of oxidizing polypyridyl metal catalysts such as Ru(bpz)<sub>3</sub><sup>2+</sup> or Ir[dF(CF<sub>3</sub>)ppy]<sub>2</sub>(dtbbpy)<sup>+</sup> led to only a trace amount of the aldehyde product, and a large amount of the alcohol remained in solution. The use of more oxidizing organophotocatalysts, including [Mes-Acr-Me]<sup>+</sup>, 2,4,6-triphenylpyrylium or DDQ resulted in a

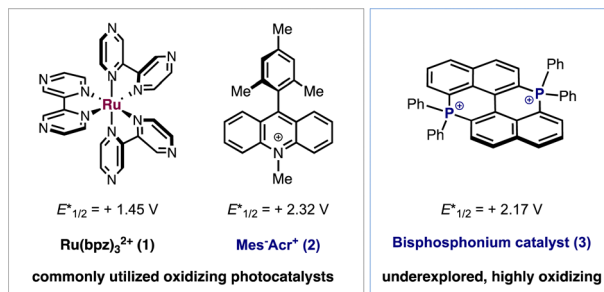
<sup>a</sup> School of Physical Science and Technology, ShanghaiTech University, Shanghai 201210, China

<sup>b</sup> State Key Laboratory of Organometallic Chemistry, Shanghai Institute of Organic Chemistry, Chinese Academy of Sciences, Shanghai 200032, China.  
 E-mail: zuozhw@sioc.ac.cn

<sup>c</sup> Innovation Center for Chenguang High Performance Fluorine Material, Key Laboratory of Green Chemistry of Sichuan Institutes of Higher Education, Sichuan University of Science and Engineering, Zigong, CN 643000, China

 † Electronic supplementary information (ESI) available. See DOI: <https://doi.org/10.1039/d3cc00532a>

‡ These authors contributed equally to this work.



## Selective oxidation of alcohols via the synergistic bisphosphonium and Co-catalysis

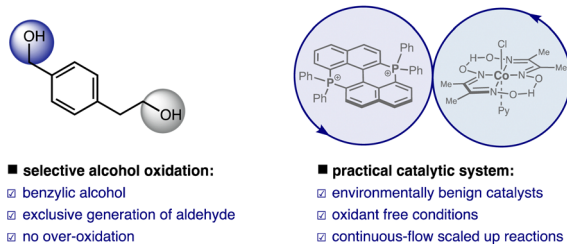
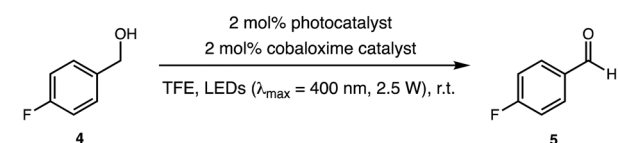
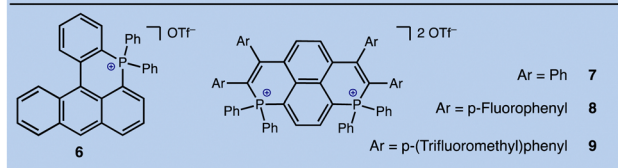


Fig. 1 Photocatalytic selective oxidation of benzylic alcohols via synergistic bisphosphonium and cobalt catalysis.



entry	photocatalyst	yield <sup>a</sup>
1	none	0% (99%)
2	Ru(bpz) <sub>3</sub> (BARF) <sub>2</sub>	2% (90%)
3	Ir[dF(CF <sub>3</sub> )ppy] <sub>2</sub> (dtbbpy)PF <sub>6</sub>	2% (98%)
4	[Mes-Acr-Me] <sup>+</sup> ClO <sub>4</sub> <sup>-</sup>	5% (95%)
5	2,4,6-triphenylpyrylium	17% (83%)
6	2,3-dichloro-5,6-dicyanobenzoquinone (DDQ)	5% (96%)
7	3	98% (90 <sup>b</sup> )
8	6	trace (100%)
9	7	3% (85%)
10	8	4% (90%)
11	9	50% (57%)
12	3, without light	0% (100%)


 Fig. 2 Reaction optimization via the evaluation of photocatalysts. Reactions were run at a 0.2 mmol scale for 6 h at room temperature under an argon atmosphere. <sup>a</sup>Yields determined via GC-FID, and the alcohol recovery is presented in parentheses. <sup>b</sup>Isolated yield.

slight improvement of the catalytic efficiency. In striking contrast, the utilization of bisphosphonium catalyst 3 enabled the full conversion of benzylic alcohol 4 to benzaldehyde 5 with 98% yield. Importantly, the possible generation of benzoic acid was

examined under scrutiny and ruled out *via* GCMS and <sup>1</sup>H NMR, validating the high selectivity of aldehyde production. Several other types of cationic P-containing conjugated arene were evaluated and compared side by side with catalyst 3. Phosphonium salt 6 ( $E^*_{1/2} = 1.64\text{ V vs. SCE}$ ), which was previously reported to exhibit intense fluorescence in aqueous medium,<sup>36,37</sup> failed to deliver any desired product in this case. Bisphosphopyrenium salts (7–9), which possess the dicationic P-containing motif with close resemblance to bisphosphonium salt 3, were also tested,<sup>38,39</sup> and only the salt with electron-deficient arene substitution (9,  $E^*_{1/2} = 2.12\text{ V vs. SCE}$ ) exhibited a moderate catalytic efficiency. These results further indicated the importance of the high oxidative capacity of bisphosphonium 3 ( $E^*_{1/2} = 2.17\text{ V vs. SCE}$ ). Moreover, control experiments revealed the critical role of light and photocatalysts.

With the environmentally benign catalysts and operationally simple conditions in hand, the reaction scope was further investigated. As exhibited in Fig. 3, a variety of primary and secondary benzylic alcohols can be oxidized to the corresponding carbonyl products smoothly using bisphosphonium catalyst 3 and the cobaloxime catalyst. Importantly, the seemingly trivial influence of the electronic properties of the benzylic motif on the catalytic efficiency was observed, as both electronically donating groups such as *p*-alkyl (12) and *p*-methoxyl (14) as well as electronically withdrawing groups such as *p*-chloro (19 and 31), *p*-fluoro (25) and 3,4-dichloro (20) can be well-tolerated. Furan and benzofuran, which are particularly prone to degradation under oxidative conditions, can also be tolerated in this oxidant-free photocatalytic transformation (products 22 and 28). Critically, in the cases of 23 and 30 where two different hydroxyl groups were presented in the same molecule, only the benzylic hydroxyl group was selectively oxidized and the primary hydroxyl group distal to the phenyl ring was left intact. Furthermore, the allylic alcohol with a conjugated phenyl substitution can be converted to the corresponding carbonyl product 32.

To further evaluate the synthetic potential of this synergistic bisphosphonium/Co catalytic system, scaled up reactions in an easily-assembled continuous-flow setup were conducted (Fig. 3). Due to the photon absorption and utilization efficiency in scaled-up vessels, photocatalytic transformations oftentimes can suffer from low conversions at the larger scale, posing significant limitations on synthetic applications. The fast conversion rate (most substrates can reach full conversion in 2 hours) and the homogeneous dispersion of all components in the TFE solvent enabled a smooth transfer from batch conditions to continuous-flow conditions, without the need for any further optimization of the catalysts. With a commonly occurring PTFE tubing coil used as the photoreactor, a series of benzaldehydes and aromatic ketones can be easily prepared at production rates of  $\sim 5\text{--}13\text{ mmol day}^{-1}$  with satisfactory yields.

Primary mechanistic investigations shed some light on the mechanism of this synergistic catalytic system (Fig. 4). Stern–Volmer quenching experiments between *p*-methoxybenzylic alcohol and photocatalyst 3 indicated a feasible photoinduced

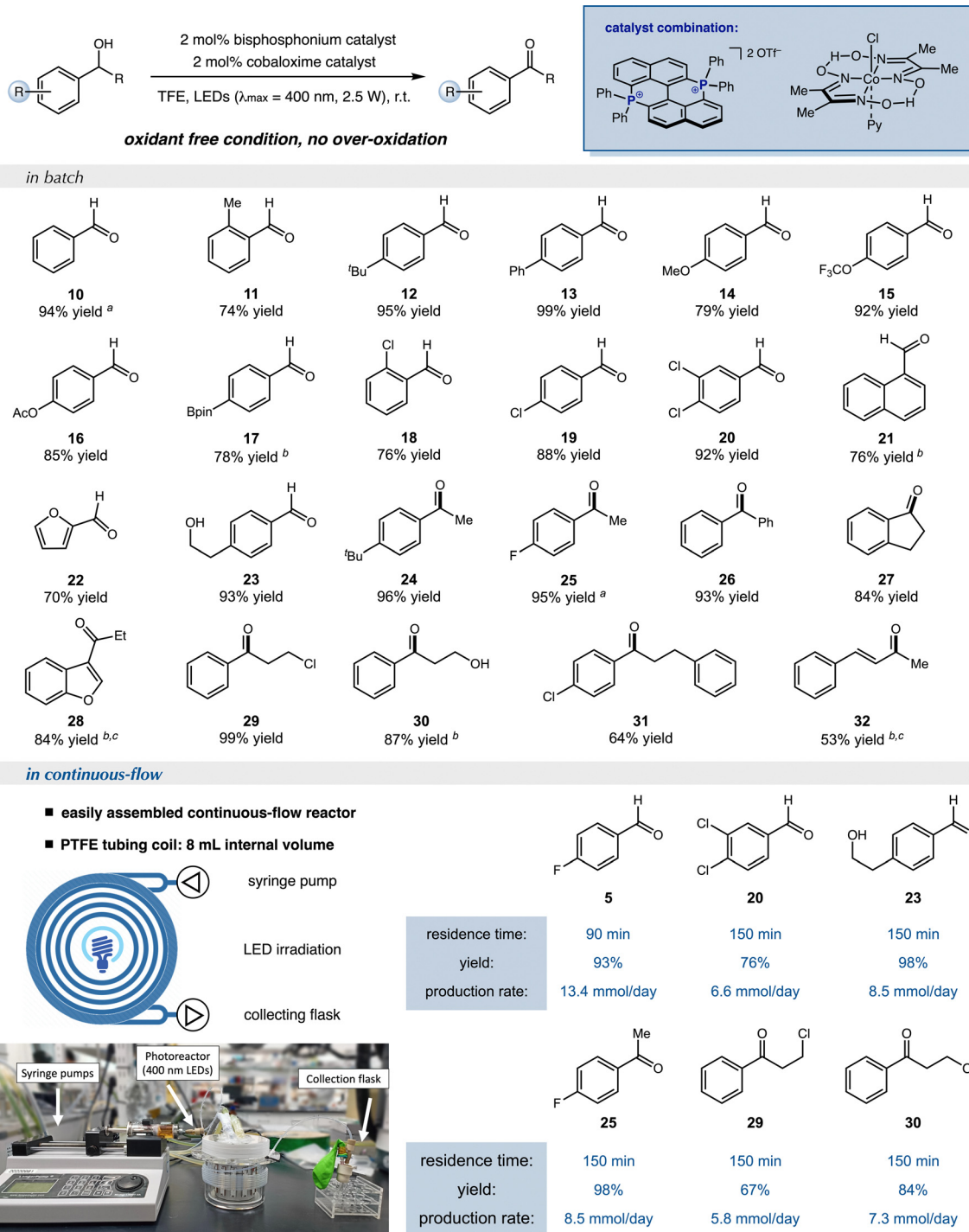


Fig. 3 Reaction scope. Batch reactions were performed at the 0.2 mmol scale, and isolated yields are shown. <sup>a</sup>Yields were determined via GC-FID due to volatile products. <sup>b</sup>4 mol% bisphosphonium **3** and 4 mol% cobaloxime were used. <sup>c</sup>MeCN was used instead of TFE. See ESI† for experimental details.

single electron transfer (SET) event which will oxidize the arene to the corresponding radical cation intermediate. Furthermore, kinetic isotope experiments with PhCH<sub>2</sub>OH and  $\alpha$ -deuterated PhCD<sub>2</sub>OH conducted in different vessels revealed a large primary KIE of 2.1, whereas the same set of KIE experiments with PhCH<sub>2</sub>OH and PhCH<sub>2</sub>OD rendered a KIE of 1.1. Intermolecular competition KIE experiments with a 1 : 1 ratio of PhCH<sub>2</sub>OH and

PhCD<sub>2</sub>OH in the same vessel, as well as intramolecular competition experiments with PhCHDOH, indicated a primary KIE of 2.0. These results unambiguously validate the cleavage of the  $\alpha$ -C-H bond of benzylic alcohol as the turnover limiting step. Furthermore, kinetic analysis revealed first order kinetics in catalyst **3** as well as in Co<sup>III</sup>(dmgH)<sub>2</sub>pyCl at low concentration. Based on these observations, we propose that the oxidation

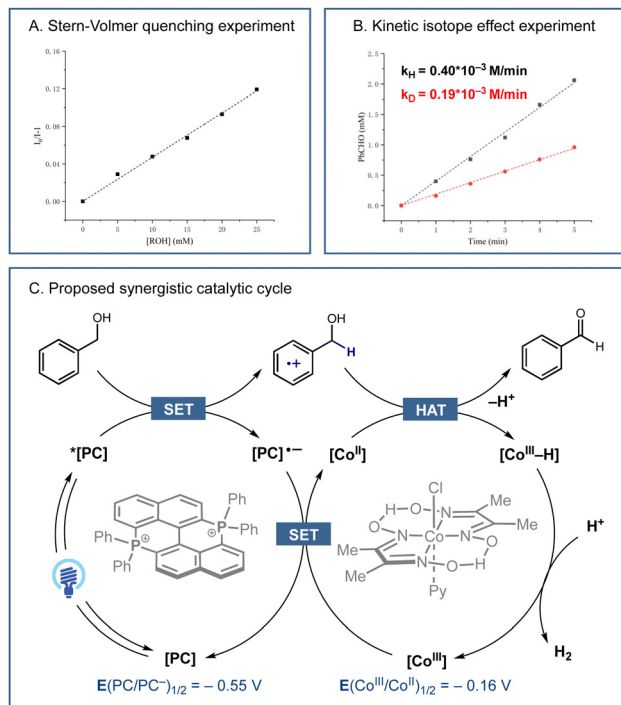


Fig. 4 (A and B) Mechanistic investigations, and (C) proposed catalytic cycle.

process starts *via* SET between the benzylic alcohol and photo-excited **3**, which will generate a radical cation intermediate with a weakened benzylic C–H bond. Subsequent Co-mediated hydrogen atom transfer will deliver the desired carbonyl product after deprotonation. The resultant  $[\text{Co}^{\text{m}}-\text{H}]$  complex then reacts with  $\text{H}^+$  to release  $\text{H}_2$ . Finally, SET between the reduced radical anion **3** ( $E_{1/2} = -0.55$  V vs. SCE) and  $[\text{Co}^{\text{III}}]$  ( $E_{1/2} = -0.16$  V vs. SCE) completes both catalytic cycles. This synergistic bisphosphonium/Co catalytic system enables the selective oxidation of benzylic alcohols under batch as well as continuous-flow conditions.

## Conflicts of interest

There are no conflicts to declare.

## Notes and references

- N. A. Romero and D. A. Nicewicz, *Chem. Rev.*, 2016, **116**, 10075–10166.
- T. Baumgartner and R. Réau, *Chem. Rev.*, 2006, **106**, 4681–4727.
- T. Baumgartner, *Acc. Chem. Res.*, 2014, **47**, 1613–1622.
- M. P. Duffy, W. Delaunay, P. A. Bouit and M. Hissler, *Chem. Soc. Rev.*, 2016, **45**, 5296–5310.
- S. O. Jeon and J. Y. Lee, *J. Mater. Chem.*, 2012, **22**, 4233–4243.
- P. Federmann, H. K. Wagner, P. W. Antoni, J. M. Morsdorf, J. L. Perez Lustres, H. Wadepohl, M. Motzkus and J. Ballmann, *Org. Lett.*, 2019, **21**, 2033–2038.

- A. Belyaev, P. T. Chou and I. O. Koshevoy, *Chem. – Eur. J.*, 2020, **27**, 537–552.
- T. Delouche, A. Vacher, T. Roisnel, M. Cordier, J.-F. Audibert, B. Le Guennic, F. Miomandre, D. Jacquemin, M. Hissler and P.-A. Bouit, *Mater. Adv.*, 2020, **1**, 3369–3377.
- E. Regulska and C. Romero-Nieto, *Mater. Today Chem.*, 2021, **22**, 100604.
- S. Nieto, P. Metola, V. M. Lynch and E. V. Anslyn, *Organometallics*, 2008, **27**, 3608.
- H. Cheng, X. Wang, L. Chang, Y. Chen, L. Chu and Z. Zuo, *Sci. Bull.*, 2019, **64**, 1896–1901.
- Z. Yang, J. Chen and S. Liao, *ACS Macro Lett.*, 2022, **11**, 1073–1078.
- X. Zhang, Y. Jiang, Q. Ma, S. Hu and S. Liao, *J. Am. Chem. Soc.*, 2021, **143**, 6357–6362.
- J. Twilton, C. Le, P. Zhang, M. H. Shaw, R. W. Evans and D. W. C. MacMillan, *Nat. Rev. Chem.*, 2017, **1**, 0052.
- I. Borthakur, A. Sau and S. Kundu, *Coord. Chem. Rev.*, 2022, **451**, 214257.
- C. Gunanathan and D. Milstein, *Science*, 2013, **341**, 1229712.
- R. H. Crabtree, *Chem. Rev.*, 2017, **117**, 9228–9246.
- Q.-Y. Meng, J.-J. Zhong, Q. Liu, X.-W. Gao, H.-H. Zhang, T. Lei, Z.-J. Li, K. Feng, B. Chen, C.-H. Tung and L.-Z. Wu, *J. Am. Chem. Soc.*, 2013, **135**, 19052–19055.
- Y.-W. Zheng, B. Chen, P. Ye, K. Feng, W. Wang, Q.-Y. Meng, L.-Z. Wu and C.-H. Tung, *J. Am. Chem. Soc.*, 2016, **138**, 10080–10083.
- G. Zhang, X. Hu, C.-W. Chiang, H. Yi, P. Pei, A. K. Singh and A. Lei, *J. Am. Chem. Soc.*, 2016, **138**, 12037–12040.
- L. Niu, H. Yi, S. Wang, T. Liu, J. Liu and A. Lei, *Nat. Commun.*, 2017, **8**, 14226.
- B. Chen, L.-Z. Wu and C.-H. Tung, *Acc. Chem. Res.*, 2018, **51**, 2512–2523.
- X. Hu, G. Zhang, F. Bu, X. Luo, K. Yi, H. Zhang and A. Lei, *Chem. Sci.*, 2018, **9**, 1521–1526.
- H. Cao, H. Jiang, H. Feng, J. M. C. Kwan, X. Liu and J. Wu, *J. Am. Chem. Soc.*, 2018, **140**, 16360–16367.
- A. Wimmer and B. König, *Adv. Synth. Catal.*, 2018, **360**, 3277–3285.
- J. B. McManus, J. D. Griffin, A. R. White and D. A. Nicewicz, *J. Am. Chem. Soc.*, 2020, **142**, 10325–10330.
- M. Kojima and S. Matsunaga, *Trends Chem.*, 2020, **2**, 410–426.
- L. Huang, T. Ji, C. Zhu, H. Yue, N. Zhumabay and M. Rueping, *Nat. Commun.*, 2022, **13**, 809.
- X. Wang, Y. Li and X. Wu, *ACS Catal.*, 2022, **12**, 3710–3718.
- K. Ohmatsu and T. Ooi, *Nat. Synth.*, 2023, **2**, 209–216.
- L.-M. Zhao, Q.-Y. Meng, X.-B. Fan, C. Ye, X.-B. Li, B. Chen, V. Ramamurthy, C.-H. Tung and L.-Z. Wu, *Angew. Chem., Int. Ed.*, 2017, **56**, 3020–3024.
- X.-J. Yang, Y.-W. Zheng, L.-Q. Zheng, L.-Z. Wu, C.-H. Tung and B. Chen, *Green Chem.*, 2019, **21**, 1401–1405.
- H. Fuse, H. Mitsunuma and M. Kanai, *J. Am. Chem. Soc.*, 2020, **142**, 4493–4499.
- D. Cambié, C. Bottecchia, N. J. W. Straathof, V. Hessel and T. Noël, *Chem. Rev.*, 2016, **116**, 10276–10341.
- J. L. Dempsey, B. S. Brunschwig, J. R. Winkler and H. B. Gray, *Acc. Chem. Res.*, 2009, **42**, 1995–2004.
- A. Belyaev, Y.-T. Chen, Z.-Y. Liu, P. Hindenberg, C.-H. Wu, P.-T. Chou, C. Romero-Nieto and I. O. Koshevoy, *Chem. – Eur. J.*, 2019, **25**, 6332–6341.
- Z. Yang, J. Chen and S. Liao, *ACS Macro Lett.*, 2022, **11**, 1073–1078.
- T. Delouche, A. Vacher, E. Caytan, T. Roisnel, B. Le Guennic, D. Jacquemin, M. Hissler and P.-A. Bouit, *Chem. – Eur. J.*, 2020, **26**, 8226–8229.
- T. Delouche, A. Vacher, T. Roisnel, M. Cordier, J.-F. Audibert, B. Le Guennic, F. Miomandre, D. Jacquemin, M. Hissler and P.-A. Bouit, *Mater. Adv.*, 2020, **1**, 3369–3377.